

SDUST2020 MSS: A global 1'×1' mean sea surface model determined from multi-satellite altimetry data

Jiajia Yuan^{1,2}, Jinyun Guo¹, Chengcheng Zhu^{1,3}, Zhen Li¹, Xin Liu¹, Jinyao Gao⁴

¹College of Geodesy and Geomatics, Shandong University of Science and Technology, Qingdao, Shandong, China

5 ²School of Geomatics, Anhui University of Science and Technology, Huainan, Anhui, China

³School of Surveying and Geo-Informatics, Shandong Jianzhu University, Jinan, Shandong, China

⁴Second Institute of Oceanography of MNR, Hangzhou, Zhejiang, China

Correspondence to: Jinyun Guo (jinyunguo1@126.com)

Abstract. This ~~article~~study focuses on the determination and ~~the~~ validation of a new global mean sea surface (MSS) model, ~~which is named as~~ SDUST2020 (Shandong University of Science and Technology 2020), with a grid size of 1'×1'. This new model ~~is was~~ established with a 19-year moving average method and merges multi-satellite altimetry data over a 27-year period (from January 1993 to December 2019). The data of HaiYang-2A, Jason-3, and Sentinel-3A ~~are were~~ first ingested in the SDUST2020 MSS, but not in any other global MSS model, such as the CLS15 and DTU18 MSS models. Validations, including ~~the~~ comparisons with the CLS15 and DTU18 MSS models, ~~the comparison with~~ GPS-levelled tide gauges, and ~~the comparison with~~ altimeter data, ~~are were~~ performed to estimate-evaluate the quality of the SDUST2020 MSS model, ~~and all the results~~all of which showed that the SDUST2020 MSS model is accurate and reliable. The SDUST2020 MSS dataset ~~are~~ is freely available at the site (data DOI: <https://doi.org/10.5281/zenodo.6555990>, Yuan et al., 2022).

1 Introduction

The Mean sea surface (MSS) is a relative steady-state sea level within a finite time span, ~~which has the~~ with important applications in geodesy, oceanography, and other disciplines (Andersen and Knudsen, 2009; Schaeffer et al., 2012; Andersen et al., 2018; Pujol et al., 2018; Guo et al., 2022). It is obtained by time averaging the instantaneous sea surface height (SSH) observed by an altimeter over a finite time span (Andersen and Knudsen, 2009). However, the sea level contains ocean a variety of variation information ~~about at multiple~~ time scales, such as seasonal and interannual variation. To completely separate the mean and time-varying parts of sea level, it is necessary to continuously collect SSH data in time and space. As ~~a result, it is a challenge for~~ establishing an MSS model ~~to that~~ accurately filter time-varying sea-sea-level signals and to obtain high-resolution mean SSH data within a finite time span is challenging.

Since the 1970s, continuous efforts have been made to establish an optimal~~studies of~~ MSS model ~~have never been interrupted~~ after the success of Geos-3 satellite altimetry data. Every update of the satellite altimetry data is accompanied by the establishment of ~~some~~ new MSS models. ~~Moreover, t~~The precision and grid size of the MSS model ~~are have been~~

gradually ~~improving-improved~~ and ~~enhancing-enhanced~~ with the development of ~~the~~-satellite altimetry techniques. ~~SoAs~~ ~~such~~, it can be said that the development of ~~an~~ MSS model is ~~an-the~~ epitome of the development history of satellite altimetry technology.

35 At present, only two research institutions, the Centre National d'Etudes Spatiales (CNES) and ~~the-s~~Space ~~research-Research~~ ~~center-Center~~ of the Technical University of Denmark (DTU), are ~~constantly~~-updating and publishing new MSS models. ~~For~~ ~~example,-t~~The series MSS models CNES_CLS11 (Schaeffer et al., 2012), CNES_CLS15 (Pujol et al., 2018), and CNES_CLS19 (ongoing to compute) ~~are-were~~ published by CNES, ~~and-while~~ the series MSS models DTU10 (Andersen et al., 2010), DTU13 (Andersen et al., 2015), DTU15 (Andersen et al., 2016), and DTU18 (Andersen et al., 2018) ~~are-were~~ published by DTU. Among them, CNES_CLS15 (~~abbreviation-for~~-CLS15) and DTU18 are the latest MSS models, ~~and~~ ~~which~~ have the same fundamental elements, ~~which-isincluding~~ the mean profile of Topex/Poseidon (T/P), Jason-1, and Jason-2 ~~span~~-from 1993 to 2012. They ~~all-also~~ have a grid size of $1' \times 1'$, ~~-but-However~~, the spatial coverage and altimetry data used are different. For example, the global coverage of ~~the~~ CLS15 model is 80°S — 84°N , while that of ~~the~~ DTU18 model is 90°S — 90°N . ~~The~~ CLS15 model ingests the exact repeat missions (ERM) data (T/P, Jason-1, Jason-2, ERS-2, 45 Envisat, GFO), as well as the geodetic missions (GM) data (ERS-1/GM, Jason-1/GM, Cryosat-2). Compared with CLS15, DTU18 replaces GFO data with SARAL/ERM data and ERS-1/GM data with SARAL ~~Drifting-drifting Phase-phase~~ (DP) data.

With the continuous development of satellite altimetry technology, the types and quantity of available SSH data are also 50 increasing-~~-on-On~~ the one hand, ~~it-comes~~data are obtained from altimetry satellites in orbit; on the other hand, ~~it-comes~~the data can also be obtained from the newly launched altimetry satellites. Multi-satellite altimetry data ~~will-be~~were fused to establish an MSS model over a longer time span. Among these altimeter data, ~~HaiYang-2A (HY-2A)~~HY-2A, Jason-3, and Sentinel-3A have not been ingested in any global MSS models (e.g. CLS15, ~~-and~~ DTU18). ~~In this study, T~~these altimeter data will be used together with other altimeter data (e.g. T/P, Jason-1, Jason-2, ERS-1, ERS-2, Envisat, GFO, Cryosat-2, and 55 SARAL) to establish ~~the-a~~ new global MSS model, called ~~the~~ SDUST2020 (Shandong University of Science and Technology 2020) model.

Ocean tides ~~is-are~~ one of the main sources of errors that affect ~~the quality of~~ altimetry data's quality. ~~However, A~~after tidal error correction, ~~there-is-still-a-certain~~-residual error, ~~which-remains-that~~ cannot be ignored ~~to-in~~ an MSS model (Yuan et al., 60 2020). Therefore, a new method, the 19-year (corresponding to the 18.61-year cycle signal of ocean tide) moving average method, ~~will-be~~was used ~~in the present study~~ to establish the SDUST2020 model with a grid size of $1' \times 1'$ from multi-satellite altimetry data spanning from 1993 to 2019. This new method has been proven~~ed~~ to be effective in improving the accuracy of the established MSS model ~~proposed by in~~ Yuan et al. (2020).

2 Data sources

2.1 Satellite altimetry data

The ~~M~~multi-satellite altimetry data used in this ~~paper-study are-were~~ selected from the along-track Level-2p (L2P; version_02_00) products ~~which~~ released by ~~the~~ Archiving Validation and Interpretation of Satellite Oceanographic Data (AVISO) (~~CENES, 2017~~2020). The L2P products contained~~s~~ multi-satellite altimetry data, including ERS-1, T/P, ERS-2, GFO, Jason-1, Envisat, Jason-2, Cryosat-2, HY-2A, SARAL, Jason-3, Sentinel-3A, and Sentinel-3B. They are generated by the 1 Hz ~~mono-mono~~-mission along-track altimetry data through various error corrections, data editing and quality control, unification of ~~the~~ reference ellipsoids (adjusted to have the same reference ellipsoid as T/P), and other data processing (~~CENES, 2020~~2017), which include instrumental errors, environmental perturbations (wet tropospheric, dry tropospheric and ionospheric effects), ~~the~~-ocean sea state bias, ~~the~~-tide effect (ocean tide, solid earth tide and pole tide), and atmospheric pressure (combining atmospheric correction: high frequency fluctuations of the sea surface topography and inverted barometer height correction). The effects of ocean tide for all the altimeter missions are corrected by the ocean tide model of FES2014 (Carrère et al., 2014). The purpose of data editing and quality control is to select valid measurements over the ocean with the data editing criteria. The editing criteria are defined as minimum and maximum thresholds for altimeter, radiometer and geophysical parameters (detailed in the along-track L2P products handbook). After data editing and quality control, data near the coastline with poor quality have been eliminated (CNES, 2020).

Multi-satellite altimetry data spanning from 1 January 1993 to 31 December 2019 selected from L2P products are shown in Table 1. Full-year ERM data ~~are-were~~ selected to ~~make-ensure the~~ altimeter data ~~was~~ less contaminated by ~~the~~-oceanic seasonal variability and the interannual signal after collinear adjustment (Schaeffer et al., 2012; Pujol et al., 2018). The ~~data of the~~ ERS-1/GM, Cryosat-2, Jason-1/GM, HY-2A/GM, and SRL/DP ~~data are-were~~ used to improve the spatial resolution of the MSS model. All ~~the data of the~~ ERM and GM data ~~are-were~~ jointly used to establish the SDUST2020 model.

Table 1. Multi-satellite altimetry data used in this study.

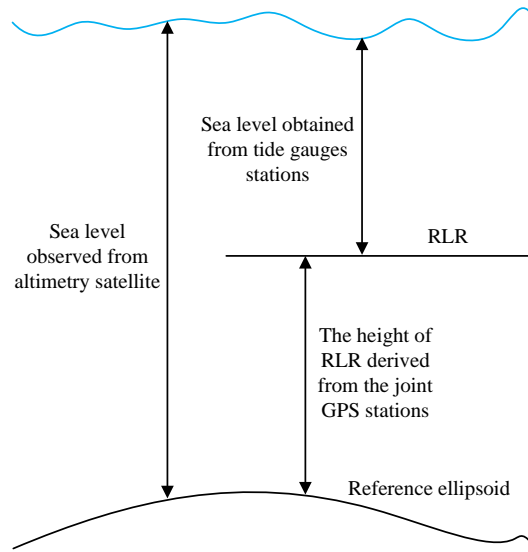
Missions	Time span	Cycles	Missions	Time span	Cycles
T/P	1993.01.01–2002.08.11	011–364	SARAL	2013.03.14–2015.03.19	001–021
Jason-1	2002.08.11–2009.01.26	022–259	HY-2A	2014.04.12–2016.03.15	067–117
Jason-2	2009.01.26–2016.10.02	021–303	Sentinel-3A	2016.06.28–2018.12.31	006–039
Jason-3	2016.10.02–2019.12.31	024–143	ERS-1/GM	1994.04.10–1995.03.21	030–040
ERS-2	1995.05.15–2003.06.02	001–084	Cryosat-2	2011.01.28–2019.12.12	014–125
GFO	2001.01.07–2008.01.18	037–208	Jason-1/GM	2012.05.07–2013.06.21	500–537
Envisat	2002.09.30–2010.10.18	010–093	HY-2A/GM	2016.03.30–2019.12.30	118–270
T/P Tandem	2002.09.20–2005.09.24	369–479	SARAL /DP	2016.07.04–2019.12.16	100–135

2.2 ~~The~~ Data of GPS-levelled tide gauges around Japan

The ~~data of~~ tide gauge ~~datas are were~~ downloaded from the Permanent Service for Mean Sea Level (PSMSL) website (www.psmsl.org/). ~~The~~ PSMSL is responsible for the collection, publication, analysis, and interpretation of ~~sea-sea~~-level data from the global network of tide gauges (Holgate et al., 2013). It provides the monthly and annual mean values for each tide gauges, ~~and these mean values have been which were~~ reduced to a common datum called Revised Local Reference (RLR) datum. This reduction ~~is was~~ performed by the PSMSL ~~making use of using~~ the tide gauge datum history provided by the supplying authority. ~~In order to~~ To avoid negative numbers in the resulting RLR monthly and annual mean values, an offset of 7000 mm ~~is was~~ also ~~made used~~.

The ~~data of~~ GPS station ~~datas are were~~ obtained from the Système d'Observation du Niveau des Eaux Littorales (SONEL) website (www.sonel.org). ~~The~~ SONEL provides the ~~URL6b-ULR6b~~ GPS daily data calculated by the University of La Rochelle (ULR) with GAMIT/GLOBK software, and the GPS data have been corrected for emergencies, such as earthquakes (Santamaria-Gomez et al., 2017).

The sea level observed ~~from by the~~ satellite altimeter ~~is was~~ relative to the reference ellipsoid. However, the sea level obtained from ~~the~~ tide gauges is relative to a certain benchmark (e.g. RLR). Therefore, there ~~are were~~ differences between these two surfaces. Fortunately, the ellipsoidal height of ~~the~~ RLR can be obtained by GPS (equipped on the tide gauges) observations, which can be used to unify the sea level obtained by the tide gauges to the reference ellipsoid. Figure 1 shows the relationship ~~among between~~ the sea level observed from the satellite altimeter ~~that is~~ relative to the reference ellipsoid, the sea level obtained from the tide gauges ~~that is~~ relative to the RLR, and the height of ~~the~~ RLR derived from GPS ~~that is~~ relative to the reference ellipsoid.



110 **Figure 1. The Relationship among-between the sea surface height (SSH) observed from altimetry satellite, the relative SSH obtained from tide gauges above the RLR (Revised Local Reference) (RLR), and the height of RLR derived from the joint GPS stations above the reference ellipsoid.**

There are about-approximately 34 tide gauges around Japan listed on the PSMSL website, which have continuous annual
 115 data spanning from 1993 to 2019 and have joint GPS data. The information of the 34 tide gauges stations and joint GPS stations around Japan are-is provide shown in the Appendix of this study. The data of-from GPS-levelled tide gauges around Japan are-were selected to validate the SDUST2020 MSS model.

3 Methodology

Figure 2 shows the data processing process-procedure used to for-establishing the SDUST2020 model. Firstly, the multi-
 120 satellite altimetry data (as-shown-in-Table 1), spanning from 1 January-1, 1993 to 31 December-31, 2019 selected from L2P products, are-were grouped into 19-year-long moving windows shifted by one year starting from-in January 1993, and then nine groups of multi-satellite altimetry data will-werebe obtained. Secondly, the multi-satellite altimetry data of each group are-were independently processed to establish a global MSS model, including the collinear adjustment of ERM data, ocean variability correction of GM data (addressed by objective analysis and polynomial fitting interpolation), multi-satellite joint
 125 crossover adjustment, and the least-squares collocation (LSC) technique for gridding. Thirdly, the-MSS models with a grid size of 1'x1' are-were established-respectively, so-resulting in nine MSS models with the same grid size-will-be-obtained. Finally, the SDUST2020 model is-was obtained by weighting the weighted average value of the nine models according to the reciprocal square of the estimated SSH error (derived from the LSC technique for gridding) at the same grid point. The calculation method is shown in equation-Equations (1) and (2):

$$mssh_{i,SDUST2020} = \frac{\sum_{j=1}^9 (mssh_{i,j}/(err_{i,j})^2)}{\sum_{j=1}^9 1/(err_{i,j})^2} \quad (1)$$

$$err_{i,SDUST2020} = \frac{1}{\sqrt{\sum_{j=1}^9 1/(err_{i,j})^2}} \quad (2)$$

where $mssh_{i,SDUST2020}$ and $err_{i,SDUST2020}$ are the SSH and the error of the SSH at the grid point i in the SDUST2020 model, respectively; $mssh_{i,SDUST2020}(j = 1, \dots, 9)$ and $err_{i,j}(j = 1, \dots, 9)$ are the SSH and the error of the SSH at the grid point i in each of the nine MSS models, respectively.

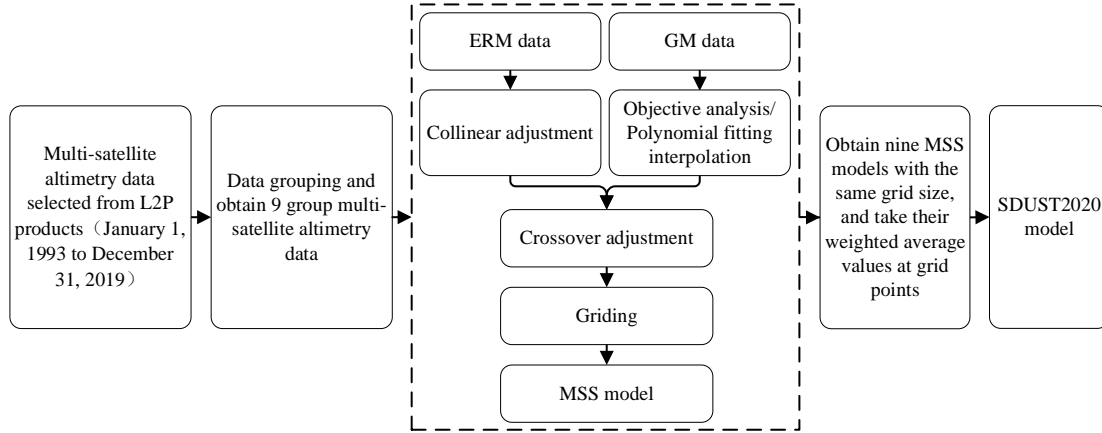


Figure 2. Data processing process of L2P products to establish the SDUST2020 model.

3.1 Ocean variability correction

The correction of altimeter data for ocean variability is a major difficulty in the process of challenge when attempting to establishing an MSS model (Schaeffer et al., 2012; Pujol et al., 2018). Since-Because the ground tracks of altimetry satellites with ERM are coinciding coincide with each other, so the ocean variability correction of ERM data can be solved by using the method of collinear adjustment method. This method makes it possible to remove the ocean variability (seasonal and interannual), but also to obtain the mean along-track SSH. The method of collinear adjustment method used in this study is the same as that described in by yuan-Yuan et al. (2021).

Since-Because the GM data does not have the characteristics of repeated periods, like-such as ERM data, so the ocean variability correction of GM data cannot be addressed by the method of collinear adjustment. Fortunately, the ocean variability of GM data has been simultaneously obtained simultaneously by using ERM data. For example, ERS-1/GM data contains the same ocean variability as the T/P data in-for the same period (1994-1995). Currently, the main methods for the correction of GM data for ocean variability are the objective analysis or based-on the use of polynomial functions (e.g. polynomial fitting interpolation, PFI). The objective analysis method is considered as-to-be the best method to correct the ocean variability of GM data (Schaeffer et al., 2012; Pujol et al., 2018); and has been applied successfully to the establishing establishment of MSS models, such as models-CLS11 and CLS15. It can be used to interpolate the ocean variability of one

or more missions considered as a reference at the spatial and temporal positions of the satellite that would be corrected for ocean variability (Schaeffer et al., 2012). The objective analysis method used in this study is described by ~~Yuan~~ Yuan et al. (2021), and further details are ~~also given in~~ provided by Le Traon et al. (1998; 2001; 2003) and Ducet et al. (2000).

~~As we all know, the~~ T/P series (refer to T/P, Jason-1, Jason-2, and Jason-3) satellite altimetry data ~~are widely known to~~ have the highest ~~measuring-measurement~~ accuracy. Therefore, the mean along-track SSH of ~~the~~ continuous T/P series during 1993–2019 are used as the ~~basis for calculating fundament to calculate~~ the ocean variability of ~~the~~ ERM data. ~~Since~~ The orbit inclination of T/P series satellites ~~are is about approximately~~ 66°, ~~while-whereas~~ that of ~~satellite with GM satellite are is~~ usually greater than 66°. For example, the orbital inclinations of ERS-1/168, HY-2A/GM, SARAL/DP, and Cryosat-2 ~~are were~~ 98.52°, 99.3°, 98.55°, and 92°, respectively. ~~So~~ Therefore, the objective analysis method can only correct the ocean variability of GM data within the latitude range of 66°S to 66°N, ~~while-whereas~~ that ~~of~~ beyond 66°S or 66°N cannot be corrected. In this study, when correcting GM data (such as ERS-1/168, HY-2A/GM, SARAL/DP and Cryosat-2) for ocean variability, ~~the-an~~ objective analysis method ~~is-was~~ adopted for ~~the~~ GM data between 66°S and 66°N, ~~while-whereas~~ the PFI method ~~is-was~~ adopted for GM data beyond 66°S or 66°N.

The basic principle of ~~method-the~~ PFI ~~method~~ can be expressed as ~~follows~~: firstly, a fitting polynomial is used to fit the grid sea level variation time series to extract the ocean variability, and the least squares solution is ~~carried-out~~ used to solve the fitting parameters; secondly, the ocean variability of GM data (above 66°S or 66°N) ~~are-is~~ interpolated with time as the independent variable, ~~so as to realize~~ the ocean variability correction of GM data. The grid sea level variation time series are ~~the~~ monthly averaged grid sea level variation time series between 1993 and 2019 provided by AVISO, with a grid of 15'×15'. The fitting polynomial ~~is-was as follows~~ (Andersen et al., 2006; Andersen and Knudsen, 2009; Jin et al., 2016):

$$y = k + bB \cdot t + cC \cdot \cos(2 \cdot \pi \cdot t) + dD \cdot \sin(2 \cdot \pi \cdot t) + eE \cdot \cos(4 \cdot \pi \cdot t) + fF \cdot \sin(4 \cdot \pi \cdot t) \quad (3)$$

where y is the ~~sea-sea~~-level variation time series; t is the time; k is the bias; $b-B$ is the trend; $c-C$ and $d-D$ are the coefficients of the annual signal; ~~and~~ $e-E$ and $f-F$ are the coefficients of the semi-annual signal.

3.2 Crossover adjustment

The crossover adjustment is an important method for the data fusion of multi-satellite altimetry (Huang et al., 2008). The ~~method-of~~ crossover adjustment ~~method used in this study is-was carried-out~~ performed in two steps: (i) ~~(1)~~-condition adjustment ~~method at crossover adjustment~~; and, (ii) ~~(2)~~-filtering and predicting of the observational corrections along each track. ~~This crossover adjustment method has been described in detail by Huang et al. (2008) and Yuan et al. (2020).~~ In the ~~process-of~~ crossover adjustment ~~process~~, an error model is established to reflect the combined effect of ~~the-systematic errors various sources of error (varied in very complicated ways)~~ on the altimeter data. These errors ~~are-include~~ the radial orbit error, residual ocean variation, residual geophysical corrections, and so on. ~~The error model can be expressed as follows~~ (Huang et al., 2008; Yuan et al., 2020; 2021):

$$f(t) = a_0 + a_1 \cdot (t - T_0) + \sum_{j=1}^n (b_j \cdot \cos(j \cdot \omega \cdot (t - T_0)) + c_j \cdot \sin(j \cdot \omega \cdot (t - T_0))) \quad (4)$$

where $f(t)$ is the systematic errors; t is the observation time of the SSH; a_0 , a_1 , b_i , and c_i ($i = 1, \dots, n$) are model parameters to be solved; ω represents the angular frequency corresponding to the duration of a surveying track ($\omega = 2\pi/(T_1 - T_0)$), where T_0 and T_1 represent the start and end times of the surveying track, respectively); and n is a positive integer determined by the length of the track. Based on empirical evidence, n is proposed to be 1–2 for a short track, 3–5 for a middle-long track, and 6–8 for a long track (Huang et al., 2008; Yuan et al., 2020).

~~Since-Because~~ the mean along-track SSH of the continuous T/P series derived from the collinear adjustment is used as the fundament-basis of the MSS model, it will remain unchanged and just-only correct crossover differences for other satellite altimetry data in the process of multi-satellite joint crossover adjustment. The details ~~about-of~~ the ~~method-of~~ crossover adjustment method used in this study are ~~given-discussed~~ in Yuan et al. (2020; 2021).

3.3 Gridding

In this study, the LSC technique (Hwang, 1989; Rapp and Bašić, 1992) ~~is-was~~ used for gridding. ~~It, which~~ has been previously proven to be the most suitable method for gridding (Jin et al., 2016). In the process of gridding with the LSC, a second-order Markov process is used to describe the two-dimensional isotropic covariance function to obtain ~~the~~-prior statistical information about the altimeter data and improve the accuracy of gridding. ~~The-This~~ process can be expressed as follows (Jordan, 1972; Moritz, 1978):

$$D(d) = D_0 \cdot (1 + d/\alpha) \cdot e^{-d/\alpha} \quad (5)$$

where d is the two-dimensional distance between the observation point and ~~the~~-grid point; D_0 is the local variance parameter, which can be expressed as the variance of all observed data participating in gridding within the local range; and α is the correlation length (where a 50% correlation is obtained). Moreover, an accuracy of $1/\sqrt{2}$ times ~~of~~ the single-satellite's crossover differences after the crossover adjustment was introduced into the LSC as the noise of the corresponding satellite data.

In the ~~process-of~~ gridding process, ~~it should be ensured that~~ the number of observation points within the range determined by the given search radius should-needs to be no less than 20, and the search radius is usually twice the grid spacing (e.g. 1'). When the number of observation points within ~~the-a~~ given searchsearch radius is less than 20, the search radius should be appropriately expanded until the conditions are met. The search method ~~is-to-ensures~~ at least five observation data points ~~at least~~ in each quadrant within the specified search range in the four quadrants centered on the grid point. The purpose of this method is to ensure that the observation data points around the grid point are uniformly distributed, which is conducive to ensuring the accuracy of grid data.

To improve the computational efficiency of gridding with the LSC, the globe ~~was~~ divided into several blocks, namely, $20^{\circ} \times 20^{\circ}$ blocks in the range of $80^{\circ}\text{S} \text{--} 60^{\circ}\text{N}$ and $0^{\circ} \text{--} 360^{\circ}$, and 126 blocks in total. In the range of $60^{\circ}\text{N} \text{--} 80^{\circ}\text{N}$ and $0^{\circ} \text{--} 360^{\circ}$, $24^{\circ} \times 20^{\circ}$ blocks ~~are were~~ divided into 18 blocks. In this way, the globe ~~is was~~ divided into ~~a total of~~ 144 blocks, of which there are only 141 blocks ~~that~~ have SSH observations; ~~while~~ two blocks ($40^{\circ}\text{N} \text{--} 60^{\circ}\text{N}$, $60^{\circ}\text{W} \text{--} 100^{\circ}\text{W}$) in the Asian continent, and one block ($40^{\circ}\text{N} \text{--} 60^{\circ}\text{N}$, $240^{\circ}\text{W} \text{--} 260^{\circ}\text{W}$) in the American continent have no SSH observations. After gridding these 141 blocks, the number of ~~the~~ 141 grids SSH data are merged. When merging, the SSH of grid points on the repeated latitude ~~lines~~ and longitude lines ~~is was~~ the SSH weighted average of grid points in the ~~two~~ adjacent ~~two~~ blocks, and the weight ~~is was~~ determined by the reciprocal of the square of the SSH error estimate at the grid points, to obtain the final gridded global MSS model.

4 Results and ~~discussion~~Discussion

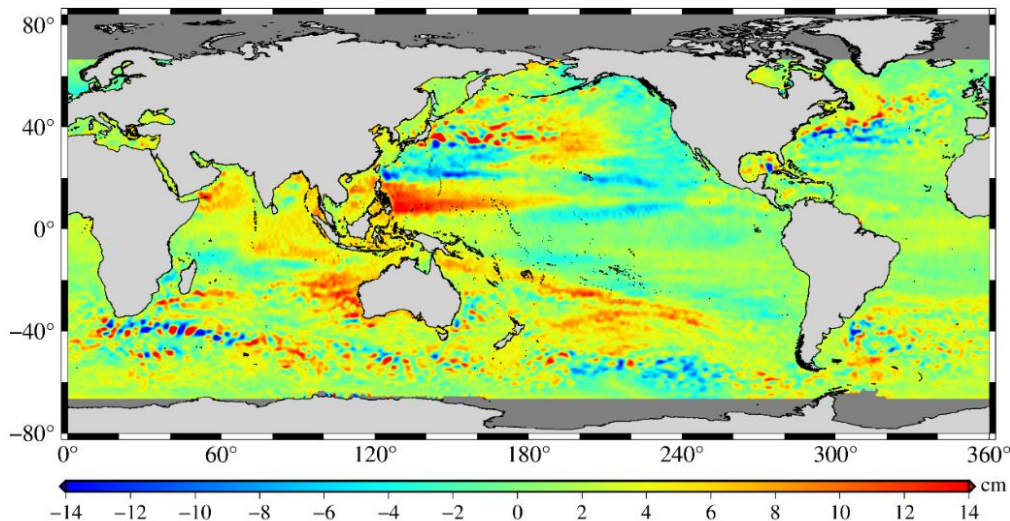
4.1 Processing results and analysis of altimetry data

Ocean variability correction can eliminate or weaken the influence of ~~sea-sea~~ level long-wave ocean variation signals, partial satellite radial orbit errors and residual errors after ~~the~~ correction of geophysical and environmental errors. Ocean variability correction ~~was~~ conducted for the altimeter missions in Table 1 in ~~the~~ global ocean, and the SSHs of these missions before and after ocean variability correction ~~are were~~ compared with ~~those of the~~ SDUST2020 model, ~~respectively~~. The statistical results of the comparisons are shown in Table 2, which shows ~~that~~ the impact of removing the ocean variability. ~~It can be seen from~~ As shown in Table 2, ~~that~~ the ~~magnitude of the RMS variance of the difference~~ (between the SSH of each satellite altimetry missions and the SDUST2020 model) ~~was reduced decrease~~ from ~~decimeterdecimetres before ocean variation correction magnitude~~ to ~~centimetercentimetres after ocean variation correction magnitude~~ RMS. Among them, ~~t~~ The RMS of ~~the~~ T/P series (T/P+Jason-1+Jason-2+Jason-3) after ocean variation correction ~~is was~~ the smallest, ~~which is~~ (0.0119 m).

Table 2. Statistical results of comparisons between heights of different altimeter missions and ~~the~~ SDUST2020 model before and after oceanic variability correction (~~Unit~~unit: m).

Missions	Before ocean variation correction			After ocean variation correction		
	Mean	STD	RMS	Mean	STD	RMS
T/P+Jason-1+Jason-2+Jason-3	0.0050	0.1038	0.1040	0.0018	0.0117	0.0119
(T/P +Jason-1) Tandem	0.0079	0.1006	0.1009	0.0029	0.0160	0.0163
ERS-2	-0.0128	0.1105	0.1112	-0.0191	0.0231	0.0300
GFO	-0.0100	0.1053	0.1057	-0.0126	0.0202	0.0238
Envisat	0.0023	0.0986	0.0986	0.0008	0.0202	0.0202
HY-2A	0.0571	0.1329	0.1446	0.0376	0.0426	0.0569
SARAL	0.0256	0.0987	0.1020	0.0220	0.0331	0.0397
Sentinel-3A	0.0437	0.0996	0.1088	0.0390	0.0318	0.0504
SARAL/DP	0.0387	0.0995	0.1068	-0.0018	0.0595	0.0595
ERS-1/GM	-0.0391	0.1075	0.1144	-0.0053	0.0676	0.0678
Jason-1/GM	0.0179	0.0978	0.0994	0.0007	0.0576	0.0576
Cryosat-2	0.0268	0.1022	0.1056	-0.0023	0.0612	0.0612
HY-2A/GM	0.0363	0.1024	0.1087	-0.0035	0.0639	0.0639

240 Figures 3 and 4 show what ~~can~~could be achieved by correcting the ocean variability of Jason-1/GM. Figure 3 shows the differences between the SSH of the Jason-1/GM and SDUST2020 model, where ~~the~~ ocean variability ~~have~~s not been corrected. Before ~~the application of applying~~ this correction, the differences ~~of in~~ SSH ~~are~~were dominant in the western boundary currents. However, these differences ~~are~~improved significantly after ~~the~~ correction ~~of for~~ ocean variability (~~as shown in~~ Figure 4).



245 Figure 3. Sea surface heights differences between Jason-1/GM and the SDUST2020 model before oceanic variability correction.

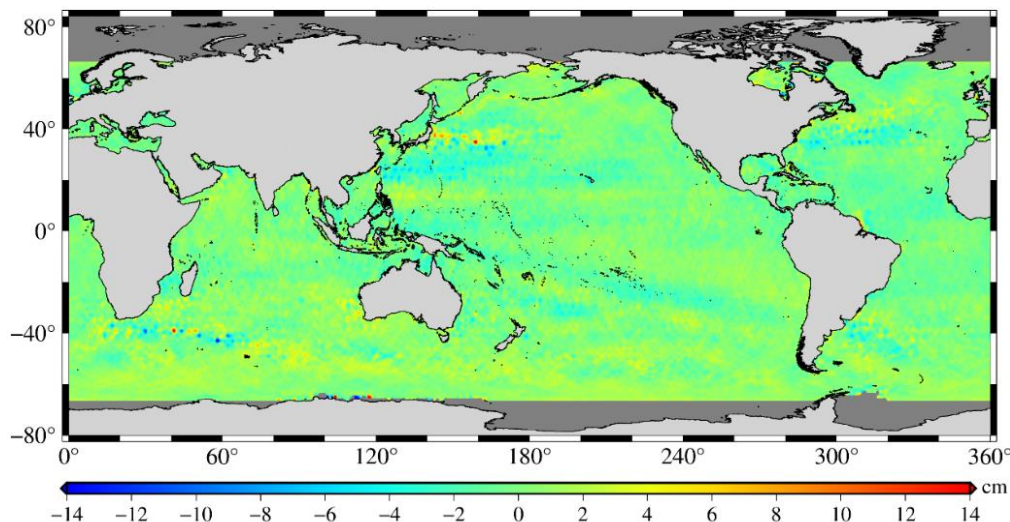


Figure 4. Sea surface heights differences between Jason-1/GM and the SDUST2020 model after oceanic variability correction.

250 All of the altimeter missions listed in Table1 ~~are~~were ~~carried out~~performed by the self-crossover adjustment respectively after ~~finishing~~completing the correction of ocean variability. Table 3 ~~shows~~presents the statistical results of the crossover

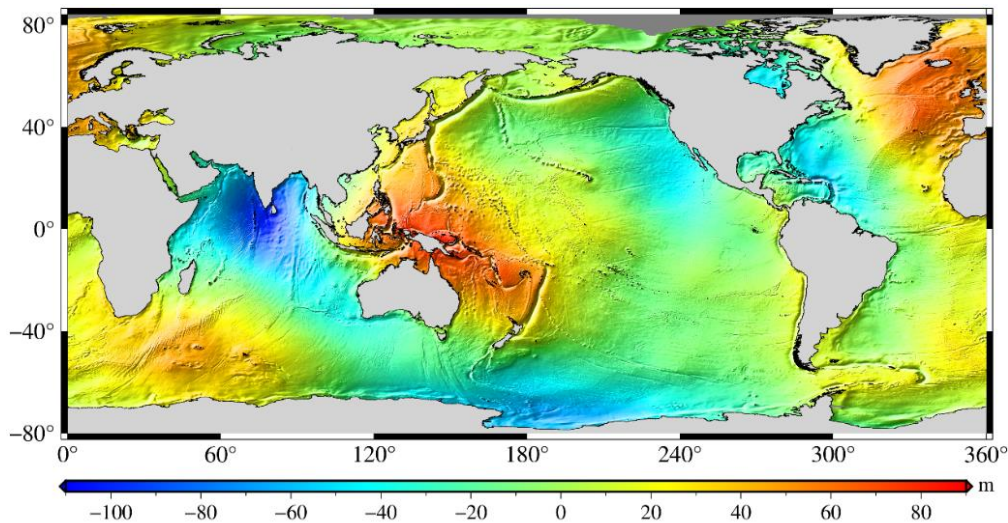
differences of these missions before and after the self-crossover adjustment. It can be seen from the results in Table 3 that the accuracy of all ~~the~~missions ~~has been was~~ greatly improved after self-crossover adjustment. The accuracy of the ERM data ~~is was~~ improved by ~~about approximately~~ 1 cm from 1–2 cm before adjustment to ~~approximately about~~ 1 cm after adjustment, ~~and while~~ that of the GM data ~~is was~~ improved by ~~approximately about~~ 2 cm from 7–9 cm to 6–7 cm. Moreover, ~~since~~ the accuracy of the ERM data (average accuracy of ~~approximately about~~ 1 cm) ~~is was~~ much higher than ~~that of the~~ GM data (average accuracy of ~~approximately about~~ 6 cm), and the accuracy of different missions ~~are was~~ also different. Therefore, the accuracy of each missions ~~will be is~~ considered in the process of multi-satellite joint crossover adjustment and ~~the~~ gridding with LSC.

Table 3. Statistical results of crossover differences of different altimeter missions before and after self-crossover adjustment (Unit: m).

Missions	Before crossover adjustment			After crossover adjustment		
	Mean	STD	RMS	Mean	STD	RMS
T/P+Jason-1+Jason-2+Jason-3	-0.0003	0.0098	0.0098	-0.0001	0.0047	0.0047
(T/P +Jason-1) Tandem	0.0001	0.0089	0.0089	0.0001	0.0060	0.0060
ERS-2	-0.0003	0.0217	0.0217	-0.0002	0.0104	0.0104
GFO	0.0003	0.0131	0.0131	0.0001	0.0077	0.0077
Envisat	0.0001	0.0208	0.0208	0.0001	0.0095	0.0095
HY-2A	0.0016	0.0238	0.0239	0.0004	0.0074	0.0075
SARAL	-0.0006	0.0219	0.0219	-0.0002	0.0134	0.0134
Sentinel-3A	-0.0001	0.0212	0.0212	-0.0001	0.0102	0.0102
SARAL/DP	0.0006	0.0835	0.0835	0.0003	0.0629	0.0629
ERS-1/GM	-0.0004	0.0899	0.0899	-0.0002	0.0708	0.0708
Jason-1/GM	-0.0015	0.0753	0.0753	-0.0008	0.0632	0.0632
Cryosat-2	0.0010	0.0824	0.0824	0.0006	0.0664	0.0664
HY-2A/GM	0.0003	0.0867	0.0867	0.0001	0.0658	0.0658

4.2 Establishment of the SDUST2020 model

According to the ~~process-procedure~~ of data processing in Figure 2, the SDUST-2020 model ~~is was~~ established ~~with using a~~ 19-year moving average method from multi-satellite altimetry data (shown in Table 1). The SDSUT2020 model is ~~shown~~ ~~illustrated~~ in Figure 5. ~~It has a with a~~ grid size of 1'×1' and a global coverage range of 80°S–84°N, with a reference time ~~spanning~~ from 1 January–1, 1993 to 31 December 31, 2019. As ~~can be seen from shown in~~ Figure 5, the global MSS ~~is was~~ generally uneven, with the highest SSH of ~~about approximately~~ 88 m and the lowest SSH of ~~approximately about~~ –106 m, with a difference of 194 m.



270 **Figure 5. Global mean sea surface model SDUST2020.**

4.3 Data availability

The SDUST2020 MSS dataset ~~as .nc file~~ is ~~now~~-available open-access at ~~the site~~ <https://doi.org/10.5281/zenodo.6555990> ~~as .nc file~~ (Yuan et al., 2022). The dataset includes geospatial information (latitude ~~and~~, longitude) and mean sea surface height.

275 **5 Comparison and validation**

~~Here, s~~Several independent ~~ways-methods are-have been~~ proposed to validate the SDSUT2020 model. Firstly, ~~we inspecting~~ ~~inspected~~ the differences ~~with another MSS models, such as CLS15 and DTU18; secondly then, we comparing-compared~~ the MSS models with the data of GPS-levelled tide gauges around Japan; ~~and finally, we comparing-compared with~~ the independent altimeter data including ~~several data-of~~ ERM and GM data.

280 **5.1 Comparison with CLS15 and DTU18 models**

The CLS15 and DTU18 models are ~~current~~-representative MSS models published by different institutions (CLS15 published by CLS and CNES; and DTU18 published by DTU). ~~In this study T~~these two models ~~are-were~~ used to validate the SDUST2020 model. Table 4 shows the information ~~of-for the~~ SDUST2020, CLS15, and DTU18 models. The main differences between SDSUT2020, ~~and~~ CLS15, and DTU18 are the reference period and ~~the~~ altimeter data ingested. The reference period of SDUST2020 ~~is-was~~ 1993-2019, while that of CLS15 and DTU18 ~~is-was~~ 1993-2012. Compared ~~with-to~~ CLS15 and DTU18, SDSUT2020 ingests more altimeter data. Among ~~these~~ altimeter data, Jason-3, HY-2A, and Sentinel-3A (ingested in the SDUST2020 model) ~~are-were~~ first used to establish an MSS model.

Table 4. Mean sea surface models SDUST2020, CLS15, and DTU18.

MSS model		SDUST2020	CLS15	DTU18
Grid size		1'×1'	1'×1'	1'×1'
Reference period		1993–2019	1993–2012	1993–2012
Coverage		80°S–84°N	80°S–84°N	90°S–90°N
Satellite ^a	ERM	T/P, J1, J2, J3, E2, EN, GFO, SA, H2A, S3A	T/P, J1, J2, E2, EN, GFO	T/P, J1, J2, E1, E2, EN, SA
	GM	E1, J1, H2A, SA, C2	E1, J1, C2	J1, C2, SA

^aFootnote: T/P for Topex/Poseidon, J1 for Jason-1, J2 for Jason-2, J3 for Jason-3, E1 for ERS-1, E2 for ERS-2, EN for Envisat, H2A for HY-2A, C2 for CryoSat-2, S3A for Sentinel-3A, SA for SARAL.

Table 5 shows the comparative statistical results of the SDUST2020, CLS15, and DTU18 models in terms of the SSH. In the comparison, the ocean variability caused by averaging over distinct periods (27 years from 1993 to 2019 for SDUST2020, and 20 years from 1993 to 2012 for CLS15 and DTU18) ~~have been was~~ removed, which ~~are was~~ calculated from the monthly averaged grid sea level variation time series between 1993 and 2019 provided by AVISO, with a grid of 15'×15'. Compared with DTU18, the STD of SDUST2020 ~~is was~~ less than that of CLS15; compared with CLS15, the STD of SDUST2020 ~~is was~~ also less than that of DTU18; ~~and while~~ compared with SDUST2020, the STD of CLS15 ~~is was~~ less than that of DTU18. Therefore, it can be inferred that the accuracy of these three models, from high to low, is SDUST2020, CLS15, and DTU18.

Table 5. Statistical results of comparisons between different mean sea surface models (Unit: m).

Model discrepancy	Max	Min	Mean	STD	RMS	Number of points
SDUST2020-CLS15	9.0319	-13.8801	0.0098	0.2083	0.2085	155330402
SDUST2020-DTU18	7.5640	-9.0388	0.0225	0.2775	0.2784	155330402
CLS15-DTU18	13.8590	-7.8108	0.0127	0.2927	0.2930	155330402

If the three models of SDUST2020, CLS15, and DTU18 are not correlated with each other, then according to the error propagation law, the STDs of these three models ~~compared with each other~~ can be expressed as follows:

$$\begin{cases} STD_{S_C}^2 = STD_S^2 + STD_C^2 \\ STD_{S_D}^2 = STD_S^2 + STD_D^2 \\ STD_{C_D}^2 = STD_C^2 + STD_D^2 \end{cases} \quad (6)$$

where STD_{S_C} , STD_{S_D} and STD_{C_D} are the STD of SDUST2020 compared with CLS15, SDUST2020 compared with DTU18, and CLS15 compared with DTU18, respectively; STD_S , STD_C and STD_D are the STD of SDUST2020, CLS15 and DTU18, respectively. According to the statistical results in Table 5, the STD of SDUST2020, CLS15 and DTU18 can be calculated ~~according to using~~ Equation (6), which are ~~about approximately~~ 0.1318 ~~m~~, 0.1613 ~~m~~ and 0.2442 ~~m~~, respectively. This result ~~can again~~ confirms that the accuracy of these three models, from high to low, is SDUST2020, CLS15 and DTU18.

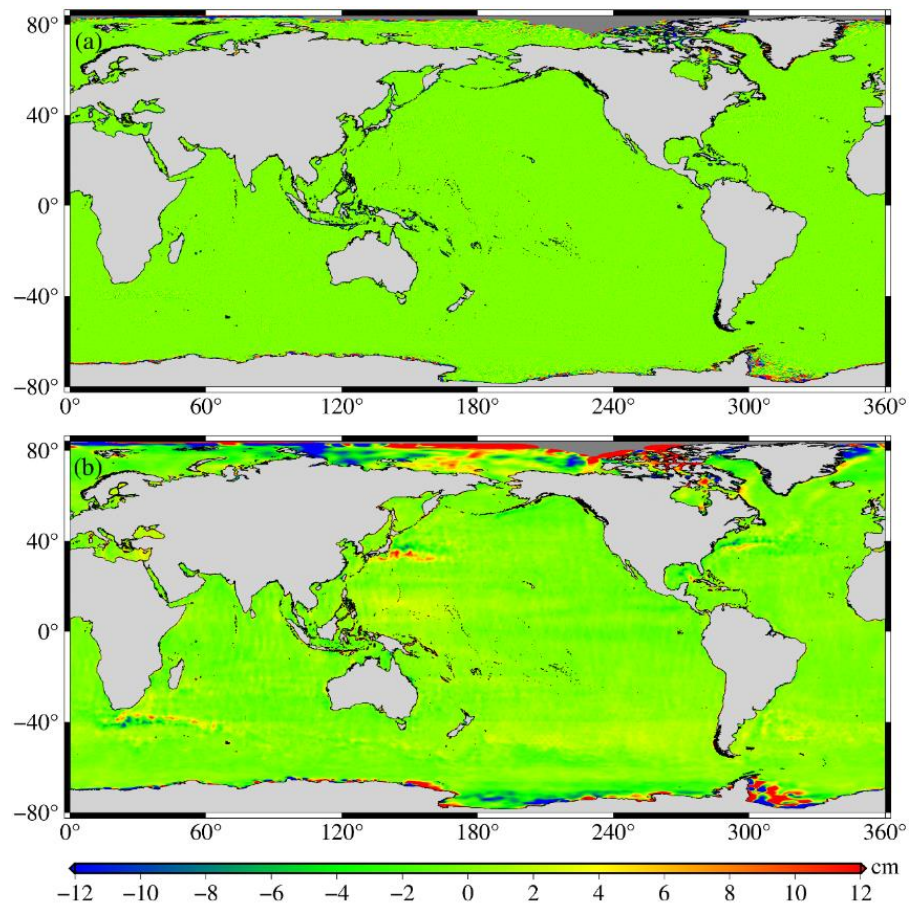
The results listed in Table 5 are the statistical results of the comparison between the three models in global ocean. A total of 1 5533 0402 grid points are counted, including grid points in the coastal regions. After outliers in the differences are rejected

by three times STD to avoid contamination by the poor observations around coastal regions, and the results are shown in Table 6. It can be inferred that the differences between the three models are around 1-2 cm, and the SDUST2020 MSS and CLS15 MSS models have the best consistency.

Table 6. Statistical results of comparisons between different mean sea surface models after rejecting outliers in differences by three times STD (unit: m).

Model discrepancy	Max	Min	Mean	STD	RMS	Number of points
SDUST2020-CLS15	0.0413	-0.0396	0.0009	0.0135	0.0135	133495409
SDUST2020-DTU18	0.0554	-0.0405	0.0074	0.0160	0.0176	131613306
CLS15-DTU18	0.0487	-0.0365	0.0060	0.0142	0.0155	129765806

The SSH differences between the SDUST2020, CLS15, and DTU18 models in the long and short wavelengths are shown in Figure 7-6 (the SSH differences between SDUST2020 and CLS15), Figure 8-7 (the SSH differences between SDUST2020 and DTU18), and Figure 9-8 (the SSH differences between CLS15 and DTU18), which ~~are~~ were drawn after a Gaussian filtering with the tools available in the GMT6.0 (Generic Mapping Tools version 6.0) software (Wessel et al., 2019). ~~As the same selected in the literature~~ Similar to Andersen et al. (2018), ~~a the~~ a wavelength of 150 km ~~is~~ was selected as the dividing line of the long and short wavelengths. ~~It can be seen from~~ As shown in the Figures 7-6, 8-7 and 9-8, ~~that there are~~ were no significant differences between these models in the short wavelength (wavelength less than 150 km), and the average differences ~~are~~ were within 2 cm, ~~while~~ whereas there ~~are~~ were some significant differences in the long wavelength (wavelengths greater than 150 km). The differences between these models ~~in the~~ at long wavelength ~~are~~ were mainly concentrated in the polar ~~circumpolar~~ regions and the western boundary current region (including the Kuroshio Current, Mexico Gulf, Agulhas Current, etc.), ~~and the sea level variation in these regions is relatively large (Jin et al., 2016). There~~ are two reasons: on the one hand, it is related to the large sea level change in these regions (Jin et al., 2016); on the other hand, it is also related to the different altimeter data used and data processing methods implemented in the modelling (Andersen and Knudsen, 2009; Schaeffer et al., 2012; Pujol et al., 2018).



335 **Figure 6. Differences between SDUST2020 and CLS15: (a) where the wavelength is less than 150 km; (b) where the wavelength is greater than 150 km.**

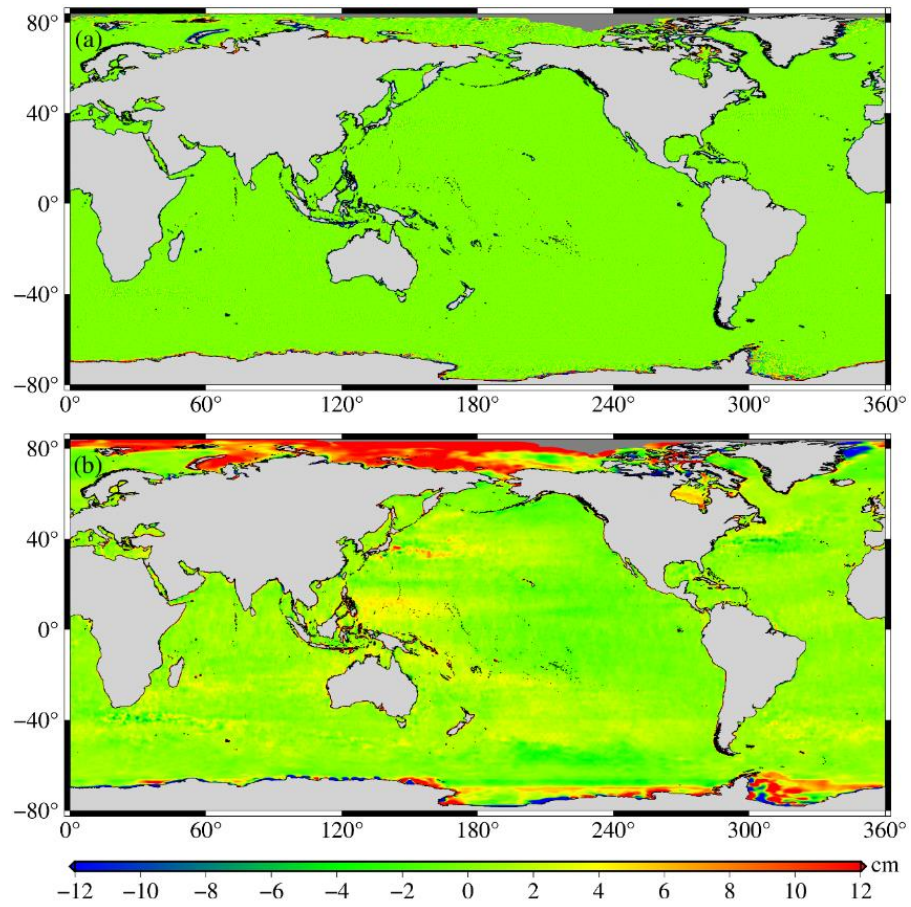


Figure 7. Differences between SDUST2020 and DTU18: (a) where the wavelength is less than 150 km; (b) where the wavelength is greater than 150 km.

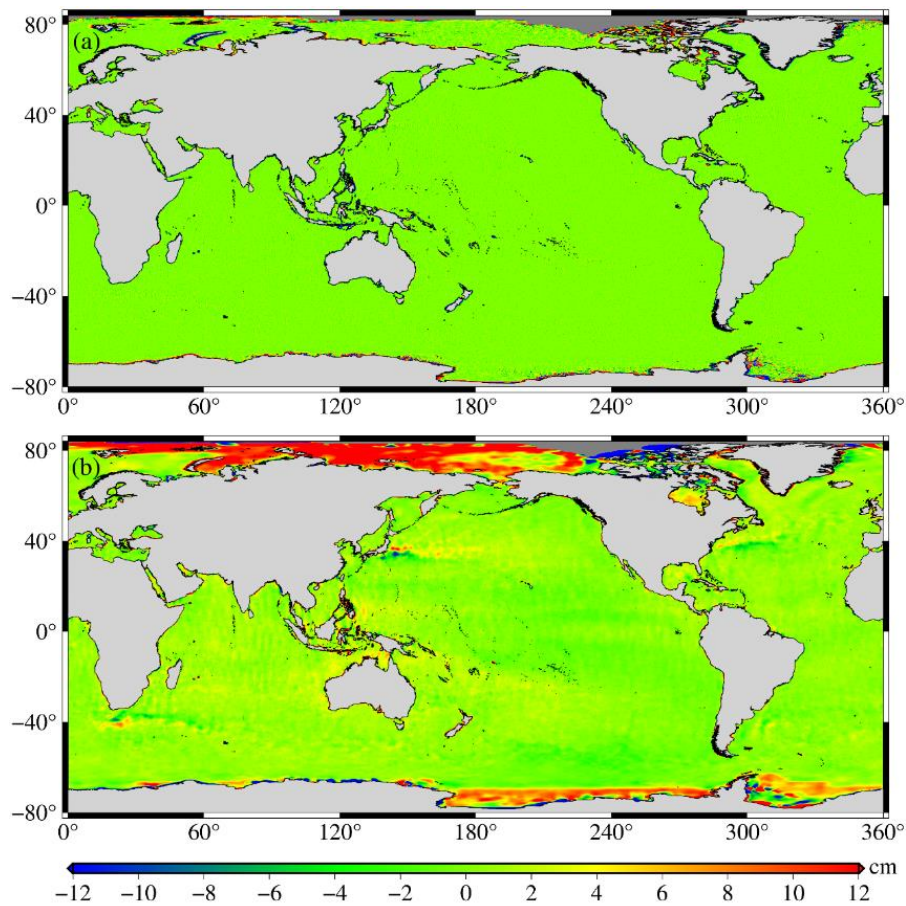
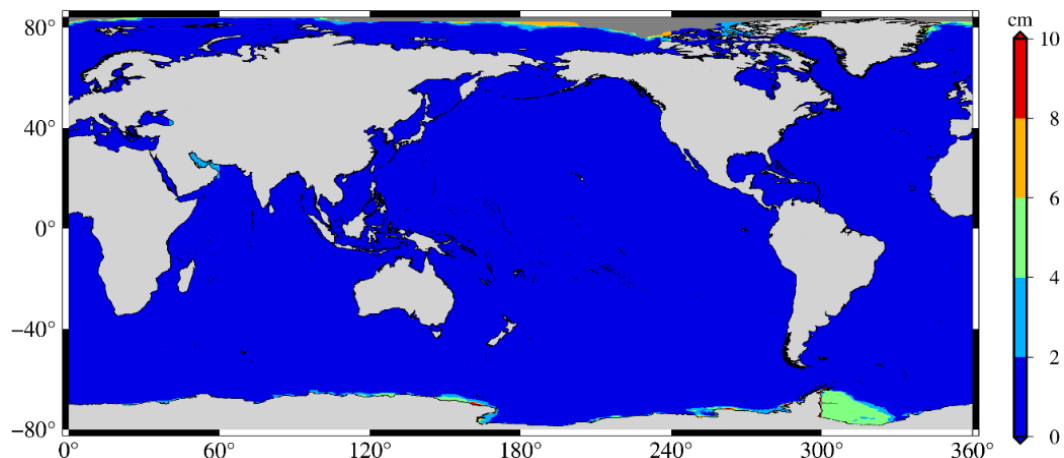


Figure 8. Differences between CLS15 and DTU18: (a) where the wavelength is less than 150 km; (b) where the wavelength is greater than 150 km.

At the optimal interpolation (using LSC technique for gridding) output, a calibrated formal error was obtained. The formal error is caused by the three terms: an instrumental noise, a residual effect of the oceanic variability, and an along-track bias. These three terms are complementary and correspond, respectively, to a white noise, a spatially correlated noise (at mesoscale wavelengths), and a long-wavelength error that is assumed to be constant along the tracks. The formal error does not match the precision of the MSS but is nonetheless an excellent indicator of the consistency of the grid (Schaeffer et al., 2012; Pujol et al., 2018).

Figures 9, 10, and 11 highlight the formal errors of SDUST2020, CLS15, and DTU18, respectively. It can be observed from these figures, which indicate that the SDUST2020 is much more homogenous and accurate than CLS15 and DTU18. This is also confirmed by the word-wide statistics. The average and RMS about the formal error of SDSUT2020 were 1.0 cm and 1.5 cm, that while those of CLS15 are 1.4 cm and 1.9 cm, and while those of DTU18 are 1.9 cm and 2.0 cm.



355 **Figure 9. Formal error of the SDUST2020 model.**

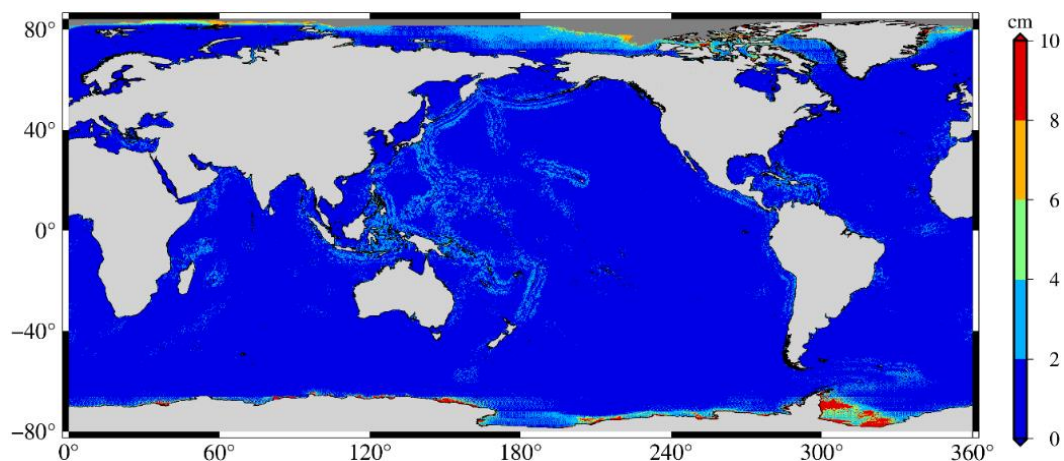


Figure 10. Formal error of the CLS15 model.

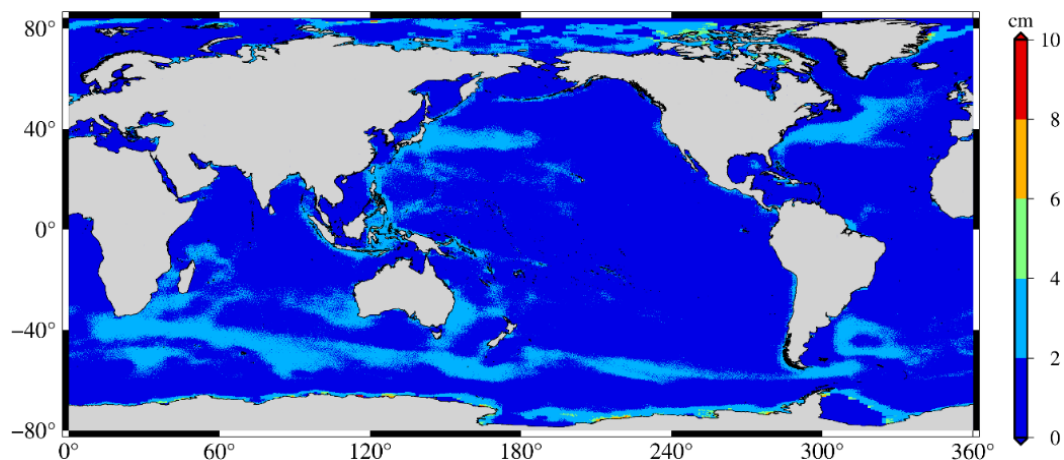


Figure 11. Formal error of the DTU18 model.

360 **5.2 Comparison with GPS-levelled tide gauges**

~~The A~~ comparison between ~~a total of~~ 34 GPS-levelled tide gauges around Japan and the SSH of ~~the~~ SDUST2020, CLS15, and DTU18 models ~~can was used to~~ independently validate the accuracy differences of ~~these~~ models ~~which that~~ are close to the coast (Andersen and Knudsen, 2009). ~~Before the comparison, the SSH obtained from the GPS-levelled tide gauges were adjusted to have the same reference ellipsoid as T/P. Since i~~It is not clear how wide ~~the~~ SSH can be represented by a single tide gauge. The SSH of different models at the location of ~~the~~ tide gauge ~~is was~~ calculated by ~~the~~ reciprocal weighting of the spherical distance from the tide gauge to the points, ~~these points are which were~~ determined by different search radii (e.g. 10 ~~km~~, 20 ~~km~~, 30 ~~km~~, 40 ~~km~~ and 50 km), which ~~are were~~ centered on the tidal station. The SSH differences of different models compared with 34 GPS-levelled tide gauges around Japan ~~in with~~ different search radii are shown in Figure 12, and ~~its their~~ STD are ~~shown listed~~ in Table 67. ~~From As shown in~~ Figure 12 and Table 67, ~~the it can be observed that the~~ larger the search radii, the greater the difference between the models and ~~the~~ GPS-levelled tide gauges. In Table 67, ~~the STD of SSHs difference between MSS model and the GPS-levelled tide gauges reaches decimeter level. The reason is may be closely related to the poor observations of offshore altimeter data. the~~The STD of ~~the~~ SSH differences of SDUST2020 compared with ~~the~~ GPS-level tide gauges are smaller than those of CLS15 and DTU18, indicating that the accuracy of SDUST2020 ~~is was~~ better than that of CLS15 and DTU18.

375 **Table 67. STD of SDUST2020, CLS15, and DTU18 models compared with GPS-levelled tide gauges around Japan in different search radii (Unit: m)**

Search radii	10 km	20 km	30 km	40 km	50 km
SDUST2020	0.1917	0.2102	0.2588	0.3264	0.3911
CLS15	0.2413	0.2296	0.2806	0.3634	0.4385
DTU18	0.2752	0.2777	0.3052	0.3512	0.4003

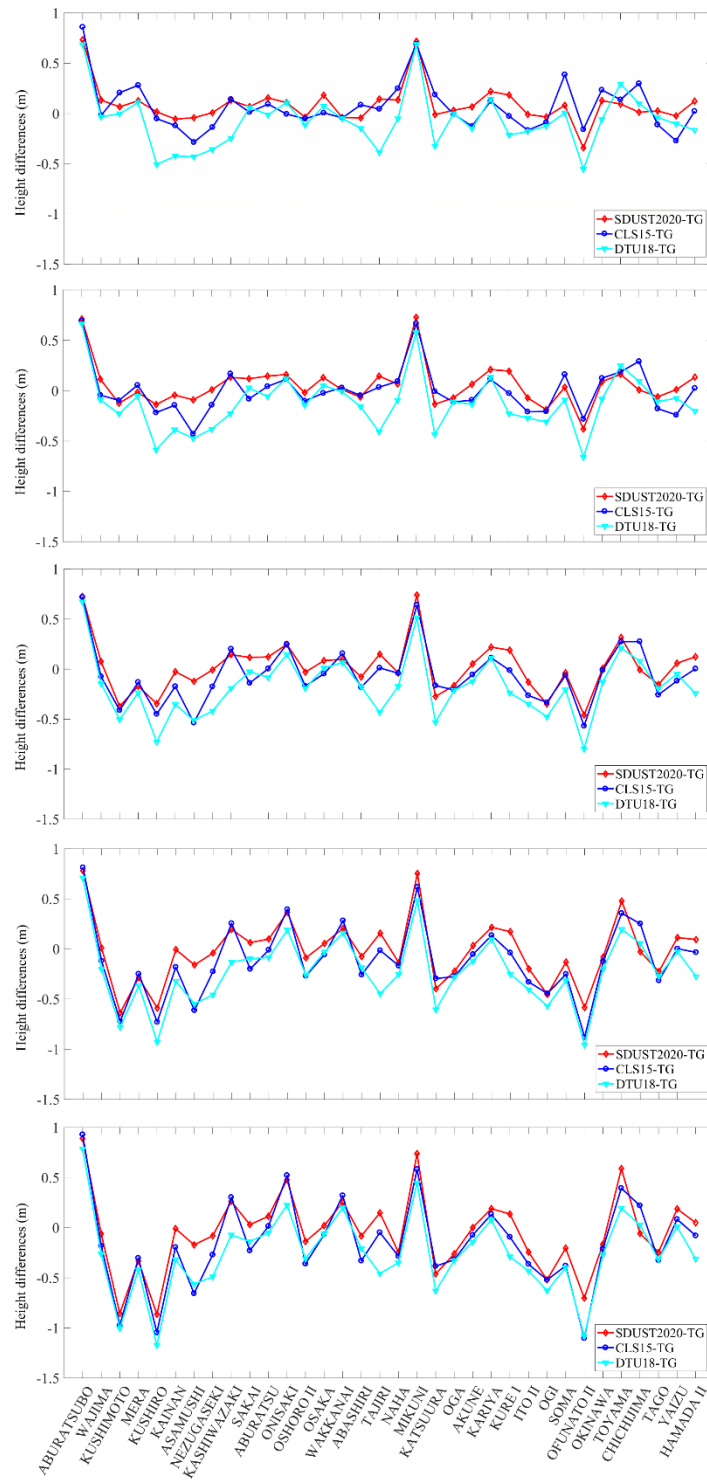


Figure 12. Sea surface height differences of different models compared with 34 GPS-levellid tide gauges around Japan in different search radius. (a), (b), (c), (d) and (e) correspond to the search radius of 10-km, 20-km, 30-km, 40-km and 50 km, respectively.

5.3 Comparison with altimeter data

The Comparison with the altimeter data can be used estimates the accuracy of the MSS models (Andersen and Knudsen, 2009; Schaeffer et al., 2012; Jin et al., 2016), which is another effective way of validating to validate the MSS models. Several datasets are were chosen, including the ERM data and GM data. The ERM data are were the mean along-track SSH after collinear adjustment, and the GM data are were not processed by ocean variability correction. The ERM data included 1-year ERS-1 data, 2-year HY-2A data, 2-year Jason-3 data, 2.5-year Sentinel-3A data and 1-year Sentinel-3B data, and the GM data included 1.5-year Envisat/GM data, 2-month Jason-2/GM data and 1-year HY-2A/GM data. Among these data, the data of Sentinel-3B and Envisat/GM are were not ingested in models of the SDUST2020, CLS15, and DTU18 models, and the data of HY-2A, Jason-3, and Sentinel-3A are were ingested in the SDUST2020 model, while they are were not ingested in the models of CLS15 and DTU18 models.

Table 7-8 shows the STD of the SSH's differences in the STD of the SSH for about the models of SDUST2020, CLS15, and DTU18 models compared with to the altimeter data. From the results in Table 78, the differences between the STD given by these three models are at in the millimeter-millimetre level, but nearly all STDs given by SDSUT2020 are lower than CLS15 and DTU18, which is an indication indicative of a higher accuracy. The STDs given by these three models are about were approximately 4-6 cm compared with the ERM data (the former five groups), approximately and about 10 cm compared with GM data (the last three groups), and the former is almost half of the later former. The This reason may be that because the altimeter data of the former five groups have been were corrected for the ocean variability, but while those of the last group have not been corrected not.

Table 78. STDs of the sea surface height differences of the models SDUST2020, CLS15, and DTU18 compared with satellite altimetry data (Unit: m).

Satellite (period)	SDUST2020	CLS15	DTU18
ERS-1 (1995.04.01-1996.04.30)	0.0529	0.0509	0.0524
HY-2A (2014.04.12-2016.03.15)	0.0565	0.0610	0.0618
Jason-3 (2017.01.01-2018.12.31)	0.0414	0.0431	0.0480
Sentinel-3A (2016.06.28-2018.12.31)	0.0448	0.0479	0.0548
Sentinel-3B (2019.01.01-2019.12.31)	0.0502	0.0522	0.0576
Envisat/GM (2010.10.27-2012.04.08)	0.0999	0.1007	0.1038
Jason-2/GM (2017.07.13-2017.09.13)	0.0991	0.0999	0.1013
HY-2A/GM (2018.12.26-2019.12.30)	0.1180	0.1187	0.1201

To more accurately assess and quantify the differences of in the model errors about for SDUST2020, CLS15, and DTU18 in at different wavelengths, the Sentinel-3B data (1-year, 2019.01.01-2019.12.31) are were selected to calculate sea level anomaly (SLA) along-track based on these three models and obtain the SLA power spectral density (PSD). Since-Because the Sentinel-3B data are were independent of these three models, the difference between the SLA PSDs of Sentinel-3B

along-track calculated based on these three models ~~reflects-reflected~~ the difference in the error of these three models (Pujol et al., 2018; Sun et al., 2021).

410 Figure 13(a) shows the mean global SLA PSD along Sentinel-3B tracks when different MSS models ~~are-were~~ used. As
shown in Figure 13(a), all PSDs ~~vary-varied~~ with the wavelengths; the longer ~~the~~ wavelengths, the greater ~~the~~ PSDs, and
there ~~are-were~~ also differences between ~~the~~ PSDs of different MSS models for different wavelengths. Since the SSH and
MSS ~~are-were~~ based on independent data and periods, it ~~can-was~~ assumed that for ~~the~~ long wavelengths (e.g. wavelengths
longer than 150 km), the ocean variability signal ~~dominates-dominated~~, for ~~the~~ short wavelengths (e.g. wavelengths from ~25
415 to 150 km), the errors of MSS models dominated, while for ~~the~~ shorter wavelengths (e.g. wavelengths shorter than 25 km),
the altimeter noise floor ~~dominates-dominated~~ (Pujol et al., 2018).

The PSD of ~~the~~ SDUST2020 model ~~is-was~~ significantly less than that of CLS15 and DTU18, and the PSD of CLS15 ~~is-was~~
slightly smaller than that of DTU18 for wavelengths longer than 150 km. The reason ~~of-for the~~ former ~~is-was~~ that the
420 reference period of SDUST2020 (1993–2019) ~~is-was~~ longer than that of CLS15 and DTU18 (1993–2012), and the reason
~~of-for thislatter is-was~~ that Sentinel-3B data uses the same data pre-processing as the altimeter data ingested in ~~the~~ CLS15
model. This ~~is-has~~ also ~~been~~ confirmed by ~~the~~ world-wide statistics. The average values of the SLA based on SDUST2020,
CLS15, and DTU18 ~~are-were~~ 0.0155 ~~-m~~, 0.0494 ~~-m~~ and 0.0596 m, respectively, and the RMS ~~values -arewere~~ 0.0525 ~~-m~~,
0.07919 ~~-m~~ and 0.0829 m, respectively.

425

Figure 13(b) shows the ratio between the PSD curves ~~of-in~~ Figure 13(a), which can better quantify the differences between
the MSS models. Compared with the CLS15 model, the errors of ~~the~~ SDUST2020 model improved in the wavelength range
from 25 to 150 km, with a maximal impact ~~around-of approximately~~ 40 km, which is ~~an~~ improved ~~ment of approximately~~ by
~~about~~ 15%.

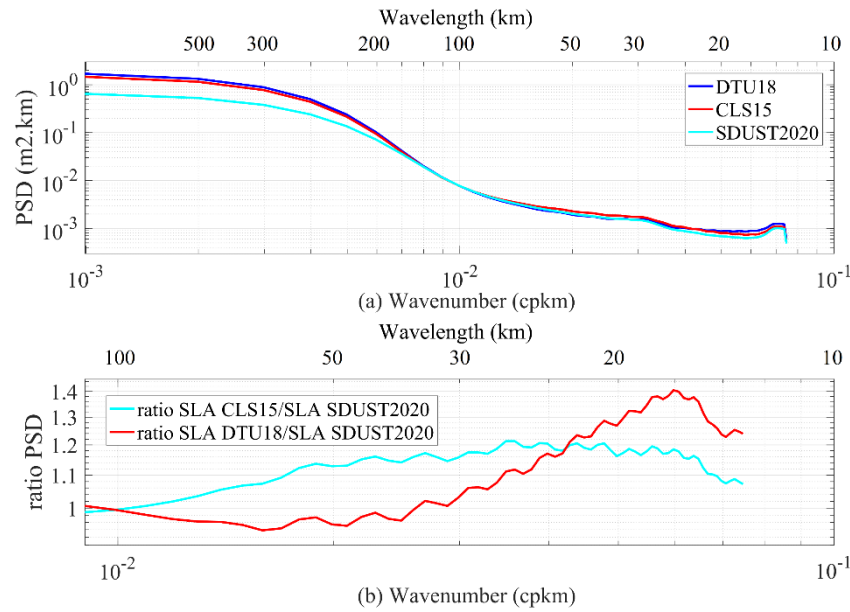


Figure 13. (a) The SLA PSD along Sentinel-3B tracks using several models. (b) The ratio of SLA PSD from panel (a).

Table 8-9 gives lists the STD about of the SLA of these three MSS models for wavelengths ranging from 25 to 150 km along different altimeter tracks. The results from As shown in Table 89, show that the accuracy difference among these three models is was very small, all in at the sub-millimeter-millimetre level, but however, the accuracy of SDUST2020 is was slightly better than that those of CLS15 and DTU18.

Table 89. STD of SLA for short wavelengths along the track of different altimeters, based on different MSS models (passband filtered from 25 to 150 km) (Unitunit: m).

	ERS-1	HY-2A	Jason-3	Sentinel-3A	Sentinel-3B	Envisat/GM	Jason-2/GM	HY-2A/GM
SDUST2020	0.0109	0.0099	0.0073	0.0089	0.0087	0.0201	0.0198	0.0205
CLS15	0.0107	0.0102	0.0067	0.0094	0.0090	0.0201	0.0198	0.0206
DTU18	0.0115	0.0107	0.0076	0.0099	0.0097	0.0202	0.0201	0.0207

6 Conclusions

In this paperstudy, SDUST2020, a new global MSS model, is was established with using a 19-year moving average method from multi-satellite altimetry data. Its global coverage is was from 80°S to 84°N with a grid size is of $1^{\circ}\times 1^{\circ}$, and a reference period is from January 1993 to December 2019.

Firstly, in Ccomparadison with the CLS15 and DTU18 models, first, the SDUST2020 model is was innovated-innovative in the data processing method of model establishment, such as usingnamely the 19-year moving average method; secondly, the reference period of the SDUST2020 model extendeded from 1993 to 2019, while that of CLS15 and DTU18 is-only ranged

from 1993 to 2012; thirdly, the establishment of the SDUST2020 model for the first time integrates the altimeter data of HY-2A, Jason-3, and Sentinel-3A, which have not been used in the establishment of any other global MSS models.

450 Comparing SDUST2020 with the CLS15 and DTU18 models, the results presented in this study show that the accuracy of these three models, from high to low, is SDUST2020, CLS15, and DTU18. Comparing SDUST2020, CLS15, and DTU18 with the data of GPS-levelled tide gauges around Japan and the altimeter data of several satellites, all these results show that the accuracy of SDUST2020 is better than that of CLS15 and DTU18.

Appendix A

455 Table A1. Information of 34 tide gauges stations and joint GPS stations around Japan.

Tide gauge	Longitude (°)	Latitude (°)	GPS station	Height of RLR (m)
ABURATSUBO	139.615278	35.160278	P108	28.874±0.012
WAJIMA	136.900278	37.405833	P111	30.416±0.015
KUSHIMOTO	135.773333	33.475833	P208	31.894±0.008
MERA	139.825000	34.918889	P206	29.398±0.009
KUSHIRO	144.371389	42.975556	P203	22.211±0.007
KAINAN	135.191389	34.144167	P117	31.220±0.007
ASAMUSHI	140.859167	40.897500	P103	30.094±0.009
NEZUGASEKI	139.545833	38.563333	P105	32.528±0.008
KASHIWAZAKI	138.508333	37.356667	P110	32.101±0.009
SAKAI	140.724722	41.781667	P204	27.380±0.009
ABURATSU	131.409444	31.576944	P211	21.404±0.013
ONISAKI	136.823611	34.903889	P116	31.038±0.014
OSHORO II	140.858056	43.209444	P101	25.709±0.013
OSAKA	129.866111	32.735000	P210	25.630±0.014
WAKKANAI	141.685278	45.407778	P201	19.991±0.008
ABASHIRI	144.285833	44.019444	P202	23.227±0.008
TAJIRI	134.315833	35.593611	P118	28.876±0.008
NAHA	127.665278	26.213333	P212	24.530±0.011
MIKUNI	136.148889	36.254722	P112	29.320±0.011
KATSUURA	140.249444	35.129444	P107	26.268±0.009
OGA	139.705833	39.942222	P104	30.603±0.007
AKUNE	130.190833	32.017500	P123	25.594±0.023
KARIYA	129.849167	33.473056	P121	25.069±0.010
KURE I	133.243333	33.333611	P120	29.147±0.010
ITO II	139.133056	34.895556	P113	33.414±0.017
OGI	138.281111	37.814722	P109	31.151±0.008
SOMA	140.962222	37.830833	P106	34.781±0.007
OFUNATO II	141.753333	39.019722	P205	33.347±0.008
OKINAWA	127.824444	26.179444	P124	23.986±0.006
TOYAMA	137.224722	36.762222	P207	31.282±0.008
CHICHIJIMA	142.183333	27.083333	P213	43.154±0.010
TAGO	138.764167	34.806944	P114	33.377±0.009
YAIZU	138.327222	34.870556	P115	33.155±0.009
HAMADA II	132.066111	34.897222	P209	26.624±0.010

Author contributions. All authors have contributed to designing the approach and writing the manuscript.

Competing interests. The contact author has declared that neither they nor their co-authors have any competing interests.

460

Disclaimer. Publisher's note: Copernicus Publications remains neutral with regard to jurisdictional claims in published maps and institutional affiliations.

Acknowledgments. We are very grateful to AVISO for providing the along-track Level-2+(L2P) products and the delayed-
465 time gridded monthly mean of sea-level anomalies product, which can be obtained by downloading freely from AVISO official website (<ftp://ftp-access.aviso.altimetry.fr>). We are also thankful to CLS for providing CNES_CLS15 MSS (<ftp://ftp-access.aviso.altimetry.fr>) and DTU for providing the DTU18 MSS (<https://ftp.space.dtu.dk/pub/>). The tide gauge records are available online (<https://www.psmsl.org/>) and the GPS data are available online (<https://www.sonel.org>).

470 **Financial support.** This work was partially supported by the National Natural Science Foundation of China (grants 42192535 and 41774001), the Autonomous and Controllable Project for Surveying and Mapping of China (grant 816517), and the SDUST Research Fund (grant 2014TDJH101).

References

- Andersen, O. B., and Knudsen, P.: DNSC08 mean sea surface and mean dynamic topography models, *J. Geophys. Res.-*
475 *Oceans*, 114(C11), 327-343, <https://doi.org/10.1029/2008JC005179>, 2009.
- Andersen, O. B., Knudsen, P., Bondo, T.: The mean sea surface DTU10 MSS-comparison with GPS and Tide Gauges, In: *ESA Living Planet Symposium*, Bergen, 2010.
- Andersen, O. B., Knudsen, P., Stenseng, L.: The DTU13 MSS (mean sea surface) and MDT (mean dynamic topography) from 20 years of satellite altimetry, In: Jin, S., Barzaghi, R. (eds) *IGFS 2014, International Association of Geodesy*
480 *Symposia*, vol 144, Springer, Cham, https://doi.org/10.1007/1345_2015_182, 2015.
- Andersen, O. B., Knudsen, P., and Stenseng, L.: A new DTU18 MSS mean sea surface–improvement from SAR altimetry, In: *25 Years of Progress in Radar Altimetry Symposium*, Portugal, 2018.
- Andersen, O. B., Vest, A. L., and Knudsen, P.: The KMS04 multi-mission mean sea surface, In: *Proceedings of the Workshop GOCINA: Improving Modelling of Ocean Transport and Climate Prediction in the North Atlantic Region Using*
485 *GOCE Gravimetry*, Novotel, Luxembourg, 13-15 April, 2006.
- Andersen, O. B., Piccioni, G., Stenseng, L., Knudsen, P.: The DTU15 MSS (mean sea surface) and DTU15LAT (lowest astronomical tide) reference surface, In: *Proceedings of the ESA Living Planet Symposium 2016*, Prague, 2016.

Carrère, L., Lyard, F., Cancet, M., Guillot, A., Dupuy, S.: FES 2014: a new global tidal model. In: OSTST Meeting, Lake Contance, Germany, 2014. http://meetings.aviso.altimetry.fr/fileadmin/user_upload/tx_ausyclsseminar/files/29Red1100-2_ppt OSTST2014 FES2014 LC.pdf.

CNES: Along-track level-2+~~h~~—(L2P) SLA product handbook. SALPMU-P-EA-23150-CLS, Issue ~~4~~2.0, https://www.aviso.altimetry.fr/fileadmin/documents/data/tools/hdbk_L2P_all_missions_except_S3.pdfhttps://www.aviso.altimetry.fr/fileadmin/documents/data/tools/hdbk_L2P_all_missions_except_S3.pdf, 20~~20~~17.

Ducet, N., Le Traon, P. Y., and Reverdin, G.: Global high-resolution mapping of ocean circulation from TOPEX/Poseidon and ERS-1 and -2, J. Geophys. Res.-Oceans, 105(C8), 19477-19498, <https://doi.org/10.1029/2000jc900063>, 2000.

Guo, J., Hwang, C., and Deng, X.: Editorial: Application of satellite altimetry in marine geodesy and geophysics, Front. Environ. Sci., 10, 910562, <https://doi.org/10.3389/feart.2022.910562>, 2022.

Holgate, S. J., Matthews, A., Woodworth, P. L., Rickards, L. J., Tamisiea, M. E., Bradshaw, E., Foden, P. R., Gordon, K. M., Jevrejeva, S., and Pugh, J.: New Data Systems and Products at the Permanent Service for Mean Sea Level, J. Coastal Res., 29(3), 493-504, <https://doi.org/10.2112/JCOASTRES-D-12-00175.1>, 2013.

Huang, M., Zhai, G., Ouyang, Y., Lu, X., Liu, C., and Wang, R.: Integrated data processing for multi-satellite missions and recovery of marine gravity field, Terr. Atmos. Ocean. Sci., 19, 103-109, [https://doi.org/10.3319/TAO.2008.19.1-2.103\(SA\)](https://doi.org/10.3319/TAO.2008.19.1-2.103(SA)), 2008.

Hwang, C.W.: High precision gravity anomaly and sea surface height estimation from Geos-3/Seasat altimeter data, M.S. Thesis. Dept. of Geodetic Science and Surveying, The Ohio State University, Columbus, OH, USA, 1989.

Jin, T., Li, J., Jiang, W.: The global mean sea surface model WHU2013, Geod. Geodyn., 7, 202-209, <http://dx.doi.org/10.1016/j.geog.2016.04.006>, 2016.

Jordan, S. K.: Self-consistent statistical models for the gravity anomaly, vertical deflections, and undulation of the geoid, J. Geophys. Res., 77(20), 3660–3670, <https://doi.org/10.1029/JB077i020p03660>, 1972.

Le Traon, P. Y., Dibarboure, G., and Ducet, N.: Use of a high-resolution model to analyze the mapping capabilities of multiple-altimeter missions, J. Atmos. Ocean. Tech., 18(7), 1277-1288, [https://doi.org/10.1175/1520-0426\(2001\)018<1277:UOAHRM>2.0.CO;2](https://doi.org/10.1175/1520-0426(2001)018<1277:UOAHRM>2.0.CO;2), 2001.

Le Traon, P. Y., Faugère, Y., Hernandez, F., Dorandeu, J., Mertz, F., and Ablain, M.: Can we merge GEOSAT follow-on with TOPEX/Poseidon and ERS-2 for an improved description of the ocean circulation?, J. Atmos. Ocean. Tech., 20(6), 889-895, [https://doi.org/10.1175/1520-0426\(2003\)020<0889:CWMGFW>2.0.CO;2](https://doi.org/10.1175/1520-0426(2003)020<0889:CWMGFW>2.0.CO;2), 2003.

Le Traon, P. Y., Nadal, F., and Ducet, N.: An improved mapping method of multisatellite altimeter data, J. Atmos. Ocean. Tech., 15(2), 522-534, [https://doi.org/10.1175/1520-0426\(1998\)015<0522:AIMMOM>2.0.CO;2](https://doi.org/10.1175/1520-0426(1998)015<0522:AIMMOM>2.0.CO;2), 1998.

Moritz, H.: Least-squares collocation, Rev. Geophys., 16(3), 421–430, <https://doi.org/10.1029/RG016i003p00421>, 1978.

Pujol, M.-I., Schaeffer, P., Faugère, Y., Raynal, M., Dibarboure, G., and Picot, N.: Gauging the improvement of recent mean sea surface models: a new approach for identifying and quantifying their errors, J. Geophys. Res.-Oceans, 123(8), 5889-5911, <https://doi.org/10.1029/2017JC013503>, 2018.

- Rapp, R. H., and Bašić, T.: Oceanwide gravity anomalies from GEOS-3, Seasat and Geosat altimeter data, *Geophys. Res. Lett.*, 19(19), 1979-1982. <https://doi.org/10.1029/92GL02247>, 1992.
- Santamaria-Gomez A., Gravelle M., Dangendorf S., Marcos, M., Spada, G., and Wöppelmann, G.: Uncertainty of the 20th century sea-level rise due to vertical land motion errors, *Earth. Planet. Sc. Lett.*, 473, 24-32, <https://doi.org/10.1016/j.epsl.2017.05.038>, 2017.
- Schaeffer, P., Faugère, Y., Legeais, J. F., Ollivier, A., Guinle, T., and Picot, N.: The CNES_CLS11 global mean sea surface computed from 16 Years of satellite altimeter data, *Mar. Geod.*, 35, 3-19, <https://doi.org/10.1080/01490419.2012.718231>, 2012.
- 530 Sun, W., Zhou, X., Yang, L., Zhou, D., and Li, F.: Construction of the mean sea surface model combined HY-2A with DTU18 MSS in the antarctic ocean, *Front. Environ. Sci.*, 9, 697111, <https://doi.org/10.3389/fenvs.2021.697111>, 2021.
- Wessel, P., Luis, J. F., Uieda, L., Scharroo, R., Wobbe, F., Smith, W. H. F., and Tian, D.: The generic mapping tools version 6, *Geochem. Geophys. Geosy.*, 20(11), 5556-5564, <https://doi.org/10.1029/2019GC008515>, 2019.
- 535 Yuan, J., Guo, J., Liu, X., Zhu, C., Niu, Y., Li, Z., Ji, B., and Ouyang, Y.: Mean sea surface model over China seas and its adjacent ocean established with the 19-year moving average method from multi-satellite altimeter data, *Cont. Shelf Res.*, 192(1), 104009, <https://doi.org/10.1016/j.csr.2019.104009>, 2020.
- Yuan, J., Guo, J., Zhu, C., Hwang, C., Yu, D., Sun, M., and Mu, D.: High-resolution sea level change around China seas revealed through multi-satellite altimeter data, *Int. J. Appl. Earth Obs.*, 102, 102433, <https://doi.org/10.1016/j.jag.2021.102433>, 2021.
- 540 Yuan, J., Guo, J., Zhu, C., Li, Z., Liu, X., and Gao, J.: SDUST2020 MSS: A global 1'×1' mean sea surface model determined from multi-satellite altimetry data [Data set], <https://doi.org/10.5281/zenodo.6555990>, 2022.